I&EC research
Industrial & Engineering Chemistry Research

pubs.acs.org/IECR

Article

Model Comparison of Performance, Operating and Capital Cost, and Environmental Impact for HFC-32/HFO-1234yf Mixtures as a Low Global Warming Alternative to R-410A

Clarice M. Sabolay, Lokesh S. Valluru, and Mark B. Shiflett*

Cite This: https://doi.org/10.1021/acs.iecr.5c02778

Read Online

ACCESS | Metrics & More | Article Recommendations | Supporting Information

ABSTRACT: Improving the energy efficiency and sustainability of cooling and heat pump systems requires the use of refrigerants with lower global warming potentials. This study evaluates the thermodynamic performance, cost, and environmental impact of difluoromethane (HFC-32) and 2,3,3,3-tetrafluoropropene (HFO-1234yf) mixtures as replacements for R-410A, which contains 50 wt % HFC-32 and 50 wt % pentafluoroethane (HFC-125). A vapor-compression cycle was modeled in heating and cooling modes, including subcooling, superheating, and irreversible compression. The coefficient of performance, capital and operating costs, and CO_2 emissions were calculated as functions of HFC-32 composition. Results show that blends with higher HFC-32 composition, such as R-454B (68.9 wt % HFC-32 and 31.1 wt % HFO-1234yf), and pure HFC-32 have higher energy efficiency and provide lower costs and reduced emissions relative to R-410A. R-454B also offers the highest condensation and evaporation heat transfer coefficients. Mixtures containing 50−100 wt % HFC-32 offer the best overall balance of energy efficiency and environmental performance.

INTRODUCTION

New refrigerants can offer opportunities to optimize performance, lower costs, and reduce environmental impacts in both existing and new systems. Several factors need to be considered when selecting a new refrigerant such as thermodynamic properties, operating and capital costs, toxicity, flammability, stability, materials compatibility, environmental properties, and equipment limitations. A key concern with hydrofluorocarbon (HFC) refrigerants is their high global warming potentials (GWP). Most modern air-conditioning systems use refrigerant R-410A, a blend of difluoromethane and pentafluoroethane. R-410A replaced the ozone depleting refrigerant chlorodifluoromethane (HCFC-22); however, R-410A has a high GWP and will be replaced by lower GWP alternatives such as pure HFC-32 with a 68% lower global warming potential and mixtures such as R-454B, with a 78% lower global warming potential. The search for low-GWP refrigerants is challenging due to trade-offs between performance, safety, and environmental impact. Studies have shown that viable lower GWP refrigerants can be limited, especially for medium- and high-pressure applications such as air conditioning, where volumetric capacity and efficiency are highly important,[1] see Table 1 for refrigerant properties, including GWP. This study compares the performance of HFC-32 and HFC-32/HFO-1234yf blends in both cooling and heating modes to evaluate performance, cost, and environmental impacts to determine the optimal composition for replacing R-410A.

Heating, ventilation, air-conditioning, and refrigeration (HVACR) systems account for over 50% of building energy consumption in the United States. The need to increase the efficiency of HVACR systems is paramount to reducing energy consumption and the impacts on global warming. Hydrofluorocarbons were replacements for chlorofluorocarbon (CFC) and hydrochlorofluorocarbon (HCFC) refrigerants, which were phased out according to the Montreal Protocol in 1987 due to having a high ozone depletion potential (ODP). HFCs have been used for over 30 years and were preferred by most equipment manufacturers, due to similar performance and zero ODP. The use of HFC mixtures provided opportunities to reduce equipment design changes by matching the properties of certain CFC (e.g., R-502) and HCFC (e.g., HCFC-22) refrigerants.

Hydrofluorocarbon refrigerants are estimated to contribute to approximately 8% of the world's greenhouse gas emissions.[2]

Received: July 7, 2025
Revised: November 18, 2025
Accepted: November 20, 2025

Table 1. Refrigerant Properties

refrigerant name	composition (wt %)	chemical formula	abbrev	GWP_{100}	ODP	boiling point (K)	ASHRAE flammability designation
difluoromethane	100.0	CH_2F_2	HFC-32	675[11]	0	221.15[5]	A2L[5]
2,3,3,3-tetrafluoropropene	100.0	$CH_2{=}CFCF_3$	HFO-1234yf	<1[6]	0	243.75[5]	A2L[5]
pentafluoroethane	100.0	CHF_2CF_3	HFC-125	2800[3]	0	224.15[5]	A1[5]
dichlorodifluoromethane	100.0	CCl_2F_2	CFC-12	8500[3]	0.73[5]	243.15[5]	A1[5]
1,1,1,2-tetrafluoroethane	100.0	CH_2FCF_3	HFC-134a	1,300[4]	0[8]	247.15[8]	A1[8]
chlorodifluoromethane	100.0	$CHClF_2$	HCFC-22	1500[3]	0.034[5]	232.15[5]	A1[5]
	68.9% HFC-32 31.1% HFO-1234yf		R-454B	465[11]	0[5]	222.25[5]	A2L[5]
	50.0% HFC-32 50.0% HFC-125		R-410A	2088[11]	0[5]	221.55[5]	A1[5]
	44.0% R-134a 56.0% HFO-1234yf		R-513A	573[8]	0[8]	244.85[8]	A1[8]

Although many HFCs have a lower GWP than CFCs, a concerted effort has been underway to identify lower GWP alternatives.[3] International agreements such as the American Innovation and Manufacturing (AIM) Act and the Kigali Amendment to the Montreal Protocol now require the phase down of high GWP refrigerants such as HFCs.[4] Additional guidance on refrigerant transition pathways is provided in the 2018 UNEP Refrigeraton, Air Conditioning, and Heat Pumps Technical Options Committee report.[5] Congress signed the AIM Act in 2020 to begin phasing down HFC production by 85% over the next two decades and replacing HFCs with HFO refrigerants.[4] HFOs have a lower GWP, zero ODP, and offer similar thermodynamic performance with respect to HFCs.[6] Recent theoretical analyses have shown that pure HFO refrigerants such as HFO-1234yf and HFO-1234ze(E) could closely match the energy and exergy of HFC-134a in household refrigeration systems while reducing total equivalent warming impact (TEWI), showing environmental superiority over HFC-134a.[7] These conclusions support ongoing efforts to use HFOs as more environmentally friendly alternatives to high-GWP HFC refrigerants. However, HFOs are not drop-in replacements for HFCs, as differences in their intrinsic properties (e.g., cooling capacity, combustibility, and compressor oil compatibility) require current HVACR systems to be redesigned for optimal performance.[6] To minimize equipment modifications, mixtures of HFC/HFO refrigerants offer opportunities to facilitate a rapid transition to lower GWP alternatives. For example, R-513A is an azeotropic HFO/HFC refrigerant mixture that is a low GWP replacement for HFC-134a. HFO-1234yf has an even lower global warming potential;[6] however, it is considered a mildly flammable refrigerant, therefore additional safety precautions are required for use in new equipment. R-513A contains enough HFC-134a that it is considered nonflammable and can be used in existing HFC-134a equipment. The cooling performance and energy efficiency of R-513A in chillers has been shown to be equivalent to HFC-134a.[8] Hydrocarbon refrigerants, such as HC-290, HC-600a, and HC-1270 have also been studied as low-GWP alternatives to HFO-1234yf in domestic refrigeration systems. Despite flammability concerns, these studies have shown that hydrocarbon refrigerants can offer higher thermodynamic efficiency and lower total equivalent warming impacts compared to HFCs when adhering to safety instructions.[9] Experimental investigations in small scale water-cooling applications reveal that low-GWP HFOs such as HFO-1234yf and HFO−HFC blends such as R-454C can offer favorable cooling performance and lower environmental repercussions compared to higher-GWP refrigerants such as HFC-1234a and R-404A.[10] These findings reinforce the selection of HFO-1234yf as a component in lower GWP refrigerant mixtures such as R-454B, which is already being adopted among other low-GWP replacements, such as HFC-32, for R-410A in air-conditioning and heat pump applications.[11] In this work, the thermodynamic performance for mixtures of HFC-32/HFO-1234yf are compared with the specific compositions for R-454B and R-410A to compare energy efficiency, costs, and environmental impacts. A range of operating conditions for cooling and heating modes were investigated to evaluate the effects of different condenser and evaporator temperatures. In addition, the economic and environmental impacts were investigated for a cooling and heating system having a lifetime of 20 years.

While several studies have evaluated pure HFOs, hydrocarbons, and commercial blends such as R-454C and R-513A, limited studies have explored HFC-32/HFO-1234yf mixtures in terms of thermodynamic performance, costs, and environmental impact. This work fills that gap by systematically assessing the performance under realistic heating and cooling conditions. In particular, this study highlights how varying HFC-32 composition influences system efficiency, capital and operating costs, and environmental impact. By combining both technical and economic perspectives, this work provides guidance for selecting lower-GWP refrigerants that balance performance, cost effectiveness, and regulatory requirements in the transition from R-410A.

Thermodynamic Modeling. The thermodynamic cycle for cooling and heating was modeled as a vapor-compression (VC) system. In heating mode, a heat pump extracts heat from an outdoor environment and transfers it to an indoor building space. In cooling mode, an air-conditioner removes heat from an indoor space and discharges it to an outdoor environment. In both cases, heat flows from higher to lower temperature, in alignment with the second law of thermodynamics.

There are four key components of a VC system: the compressor, condenser, evaporator, and expansion device. Three operating cases are considered. In Case 1, the most ideal scenario, compression is isentropic, expansion is isenthalpic, and both the condenser and evaporator operate isobarically, as shown in Table 2.

A pressure vs enthalpy ($P-\hat{H}$)diagram visualizing the cycle in Case 1 is shown in Figure 1 (cycle in black). Key operations

https://doi.org/10.1021/acs.iecr.5c02778
Ind. Eng. Chem. Res. XXXX, XXX, XXX−XXX

Table 2. Operating Conditions, Ideal Case 1

components	assumption(s)
compressor	isentropic—constant entropy, reversible
condenser	isobaric—constant pressure
evaporator	isobaric
expansion valve	isenthalpic—constant enthalpy

can be represented by transitions between specific state points, described in Table 3.

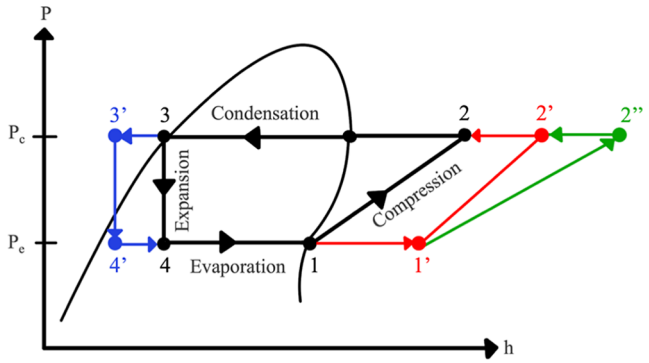

Figure 1. Pressure−Enthalpy diagram for an actual VC cycle with subcooling and superheating.

Table 3. VC Cycle State Points, Ideal Case 1

state point	operation
1 to 2	compression—low-*P* saturated vapor to high-*P* vapor
2 to 3	condensation—high-*P* vapor to high-*P* saturated liquid
3 to 4	expansion—high-*P* saturated liquid to low-*P* two-phase liquid−vapor
4 to 1	evaporation—low-*P* liquid−vapor to low-*P* saturated vapor

In Case 2, the compression is irreversible ($S_{gen} > 0$), and a new state point after compression (2′) is shown in Figure 1 (cycle in red).

In Case 3, subcooling and superheating are included. Subcooling the refrigerant below the condensing temperature (state point 3 to 3′ in Figure 1, cycle in blue), helps prevent vapor bubbles that can cause cavitation in expansion devices.[12] Superheating increases the refrigerant temperature above the evaporating temperature (state point 1 to 1′ as shown in Figure 1, cycle in green), which prevents liquid droplets from entering and damaging the compressor.[12,13]

To evaluate the energy efficiency of the system, the Coefficient of Performance (C.O.P.) was calculated using eqs 1 and 2 depending upon the operating mode

$$\text{C. O. P(Heating)} = \frac{Q_{\text{cond.}}}{W_{\text{comp.}}} = \frac{\hat{H}_{3'} - \hat{H}_{2''}}{\hat{H}_{2''} - \hat{H}_{1'}} \quad (1)$$

$$\text{C. O. P(Cooling)} = \frac{Q_{\text{evap.}}}{W_{\text{comp.}}} = \frac{\hat{H}_{1'} - \hat{H}_{4'}}{\hat{H}_{2''} - \hat{H}_{1'}} \quad (2)$$

where $Q_{cond.}$ is the condenser heat flow, and $Q_{evap.}$ is the evaporator heat flow, and $W_{comp.}$ is the compressor work. Enthalpy values (kJ·kg^{-1}) were calculated for Case 3, which includes subcooling, superheating, and irreversible compression at the state points shown in Figure 1 and eqs 1 and 2. It is important to note that the theoretical C.O.P. is highest in the ideal cycle (Case 1).

METHODOLOGY

For both heating and cooling modes, the C.O.P., operating cost, and capital cost were calculated for HFC-32/HFO-1234yf mixtures over a range of HFC-32 compositions (w_{HFC-32} = 0 to 1). The composition of commercially available R-454B (w_{HFC-32} = 0.689) was included for comparison. Cycle parameters and evaporator and condenser temperatures are provided in Table 4 and Table 5 respectively.

Table 4. VC Cycle Parameters for Heating and Cooling Modes

parameter	value
R-410A	50 wt % HFC-32/50 wt % HFC-125
R-454B	68.9 wt % HFC-32/31.1 wt % HFO-1234yf
irreversible compressor efficiency	0.8 (80%)
degrees of subcooling and superheating (ΔT)	±5 °C
condenser pressure drop	0 MPa
evaporator pressure drop	0 MPa

Table 5. Evaporator and Condenser Temperatures

heating mode	cooling mode
$T_{evap.}$ = −6.67, −1.11, 4.44 °C (20, 30, 40 °F)	$T_{evap.}$ = 4.44 °C (40 °F)
$T_{cond.}$ = 43.33 °C (110 °F)	$T_{cond.}$ = 32.22, 43.33, 54.44 °C (90, 110, 130 °F)

Thermodynamic properties for R-410A, HFC-32, HFO-1234yf, and mixtures of HFC-32 and HFO-1234yf were calculated using the NIST Reference Fluid Properties (REFPROP) program[13] at each state point. Input variables and output properties for each point are described in Table 6. Additional details on the vapor-compression cycle calculations, including example state-point data and sample C.O.P. calculations, are provided in the Supporting Information.

Table 6. State Points Calculated Using NIST REFPROP Program: Temperature (*T*, °C), Pressure (P, MPa), Enthalpy ($\hat{H}$, kJ·kg^{-1}), and Entropy ($\hat{S}$, kJ·kg^{-1} K^{-1})[a]

state points (phase)	input	calculated
1 (saturated low-*P* vapor)	*T*	*P*, $\hat{H}$, $\hat{S}$
1′ (superheated low-*P* vapor)	*T*, *P*	$\hat{H}$, $\hat{S}$
2 (high-*P* vapor)	*P*, $\hat{S}$	*T*, $\hat{H}$
3 (saturated high-*P* liquid)	*T*	*P*, $\hat{H}$, $\hat{S}$
3′ (subcooled high-*P* liquid)	*T*, *P*	$\hat{H}$, $\hat{S}$
4 (Low-*P* two-phase liquid and vapor)	*T*, $\hat{H}$	*P*, $\hat{S}$

[a]*See Supporting Information for Details.

The basis for calculating the operating cost for both heating and cooling modes is shown in Table 7.

The refrigerant mass flow rate, $\dot{m}_{mix}$ (kg·min^{-1}), for heating and cooling was calculated using eqs 3 and 4.

$$\dot{m}_{\text{mix}}\text{(Heating)} = \frac{\dot{Q}}{Q_{\text{cond.}}} \quad (3)$$

https://doi.org/10.1021/acs.iecr.5c02778
Ind. Eng. Chem. Res. XXXX, XXX, XXX−XXX

Table 7. Operating Cost Basis

basis	value
fixed heating/cooling capacity (kJ·min^{-1})	630
average U.S. electricity cost ($·kWh^{-1})	0.14
run time (hours/day)	12
days/month	30

$$\dot{m}_{mix}(\text{Cooling}) = \frac{\dot{Q}}{Q_{evap.}} \quad (4)$$

where $\dot{Q}$ is the heating or cooling capacity, $Q_{cond.}$ is the condenser heat flow, and $Q_{evap.}$ is the evaporator heat flow (see Figures S1 and S2 in Supporting Information). Power (Po, kJ·min^{-1}) was calculated using eq 5 where $W_{comp.}$ is the compressor work (kJ·kg^{-1}).

$$\text{Po} = W_{comp.} \cdot \dot{m}_{mix} \quad (5)$$

The operating cost ($\frac{\$}{\text{month}}$) was calculated using eq 6

$$\text{OC} = \frac{\$}{\text{month}} = \frac{\text{Po}}{60} \cdot \frac{\text{hours}}{\text{day}} \cdot \frac{\text{days}}{\text{month}} \cdot \frac{\$}{\text{kWh}} \quad (6)$$

where $\frac{\text{Po}}{60}$ is a conversion of power from kJ·min^{-1} to kW, $\frac{\$}{\text{kWh}}$ is the average U.S. electricity cost, $\frac{\text{hours}}{\text{day}}$ is the unit run time, and $\frac{\text{days}}{\text{month}}$ is how many days the unit runs per month.

To calculate the unit's capital cost, a manufacturer's cost (MC) of $3500 was specified for a basis size of 10.5 kW (630 kJ·min^{-1} or 3 ton) for a R-410A heat pump. The capital cost of each unit was scaled relative to refrigerant mass flow rate and compared with the basis cost for the R-410A equipment. The refrigerant flow rate ratio (FRR) is shown in eq 7, where $\dot{m}_{mix}$ is the refrigerant mass flow rate (kJ·min^{-1}) and $\dot{m}_{R-410A}$ is the R-410A mass flow rate.

$$\text{FRR} = \frac{\dot{m}_{mix}}{\dot{m}_{R-410A}} \quad (7)$$

The capital cost was calculated by multiplying the flow rate ratio by the manufacturing cost as shown in eq 8.

$$\text{C. C.} = \text{FRR} \cdot \text{MC} \quad (8)$$

The operating cost and capital cost were compared with R-410A and the difference (ΔO.C. and ΔC.C) is reported as shown in eqs 9 and 10.

$$\Delta\text{O. C.} = \text{O. C.}_{R-410A} - \text{O. C.}_{mix.} \quad (9)$$

$$\Delta\text{C. C.} = \text{C. C.}_{R-410A} - \text{C. C.}_{mix.} \quad (10)$$

RESULTS AND DISCUSSION

The C.O.P., operating cost, and capital cost for mixtures of HFC-32 and HFO-1234yf—including R-454B—were evaluated as a function of HFC-32 composition for both heating and cooling modes. Results are shown in Figures 4−9 as a function of evaporator temperature and condenser temperature.

In heating mode, the C.O.P reaches a minimum at an HFC-32 mass fraction of 0.1, then increases with higher HFC-32 composition (Figure 2). As expected, the C.O.P. also increases with increasing evaporator temperature due to a decrease in the pressure ratio between the condenser and evaporator.

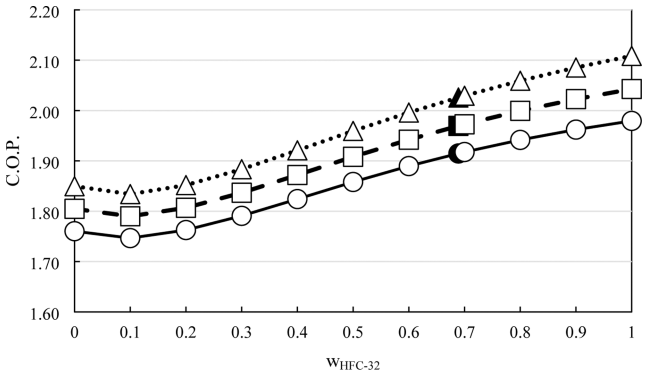

Figure 2. C.O.P as a function of HFC-32 composition and evaporator temperature (circle: $T_{evap.}$ = −6.67 °C, square: $T_{evap.}$ = −1.11 °C, triangle: $T_{evap.}$ = 4.44 °C) for heating mode at condenser temperature ($T_{cond.}$ = 43.33 °C). Solid symbols represent the composition for R-454B.

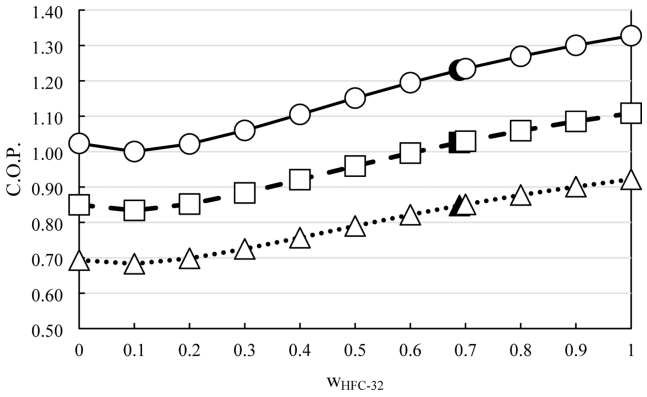

Figure 3. C.O.P as a function of HFC-32 composition and condenser temperature (circle: $T_{cond.}$ = 32.22 °C, square: $T_{cond.}$ = 43.33 °C, triangle: $T_{cond.}$ = 54.44 °C) for cooling mode at evaporator temperature ($T_{evap.}$ = 4.44 °C). Solid symbols represent the composition for R-454B.

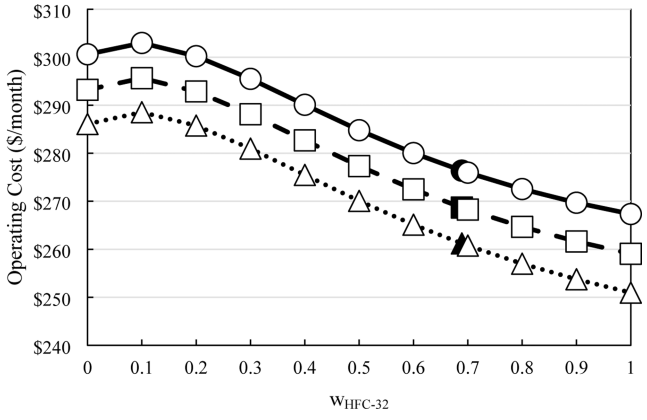

Figure 4. Operating cost ($/month) as a function of HFC-32 composition and evaporator temperature (circle: $T_{evap.}$ = −6.67 °C, square: $T_{evap.}$ = −1.11 °C, triangle: $T_{evap.}$ = 4.44 °C) for heating mode at condenser temperature ($T_{cond.}$ = 43.33 °C). Solid symbols represent the composition for R-454B.

In cooling mode, a similar trend is observed: C.O.P. is minimized at w_{HFC-32} = 0.1, then increases with higher HFC-32 compositions (Figure 3). Again, as expected, C.O.P. increases

https://doi.org/10.1021/acs.iecr.5c02778
Ind. Eng. Chem. Res. XXXX, XXX, XXX−XXX

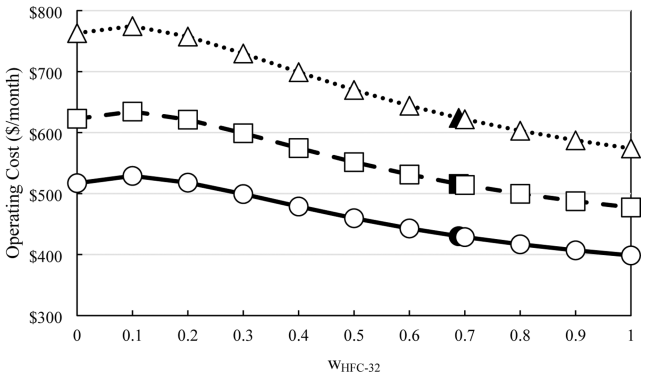

Figure 5. Operating cost ($/month) as a function of HFC-32 composition and condenser temperature (Circle: $T_{cond.}$ = 32.22 °C, Square: $T_{cond.}$ = 43.33 °C, Triangle: $T_{cond.}$ = 54.44 °C) for cooling mode at evaporator temperature ($T_{evap.}$ = 4.44 °C). Solid symbols represent the composition for R-454B.

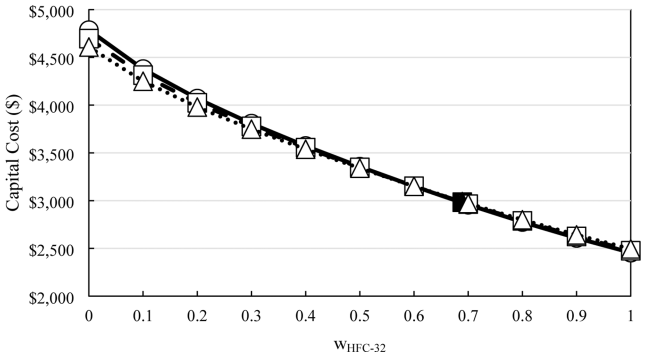

Figure 6. Capital cost ($) as a function of HFC-32 composition and evaporator temperature (Circle: $T_{evap.}$ = −6.67 °C, Square: $T_{evap.}$ = −1.11 °C, Triangle: $T_{evap.}$ = 4.44 °C) for heating mode at condenser temperature ($T_{cond.}$ = 43.33 °C). Solid symbols represent the composition for R-454B.

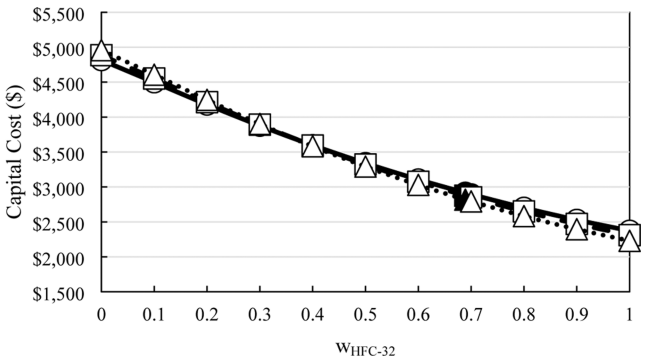

Figure 7. Capital cost ($) as a function of HFC-32 composition and condenser temperature (Circle: $T_{cond.}$ = 32.22 °C, Square: $T_{cond.}$ = 43.33 °C, Triangle: $T_{cond.}$ = 54.44 °C) for cooling mode at evaporator temperature ($T_{evap.}$ = 4.44 °C). Solid symbols represent the composition for R-454B.

as the condenser temperature decreases due to the decrease in the pressure ratio.

Operating cost, which inversely depends on C.O.P., follows a similar trend. In both heating and cooling modes, operating cost reaches a maximum at w_{HFC-32} = 0.1 and decreases as HFC-32 composition increases (Figures 4 and 5). In addition, operating cost in heating mode decreases with increasing

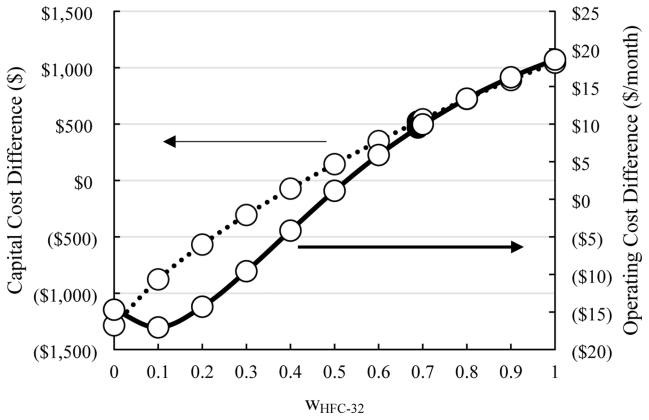

Figure 8. Capital cost difference ($, dotted line) and operating cost difference ($/month, solid line) as a function of HFC-32 composition for heating mode at evaporator temperature ($T_{evap.}$ = −6.67 °C) and condenser temperature ($T_{cond.}$ = 43.33 °C). Solid symbols represent the composition for R-454B. Positive values (no parentheses) and negative values (with parentheses).

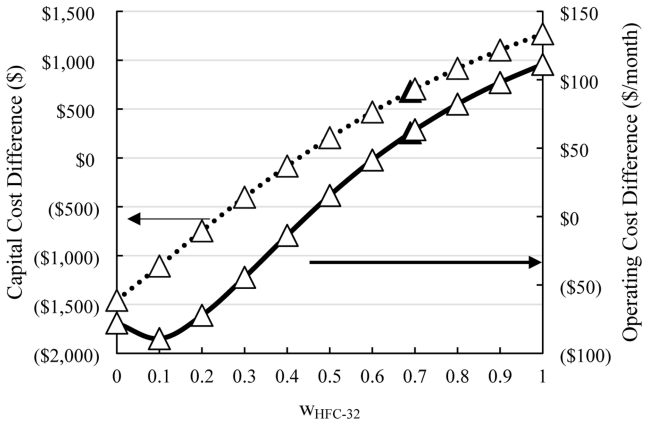

Figure 9. Capital cost difference ($, dotted line) and operating cost difference ($/month, solid line) as a function of HFC-32 composition for cooling mode at condenser temperature ($T_{cond.}$ = 54.44 °C) and evaporator temperature ($T_{evap.}$ = 4.44 °C). Solid symbols represent the composition for R-454B. Positive values (no parentheses) and negative values (with parentheses).

evaporator temperature, while in cooling mode it decreases with decreasing condenser temperature, which occurs in both cases due to a decrease in the compression ratio.

Capital cost, scaled with refrigerant mass flow rate, also decreases with increasing HFC-32 composition in both heating and cooling modes (Figures 6 and 7). In heating mode, capital cost further decreases with higher evaporator temperatures. In cooling mode, it decreases with lower condenser temperatures at low HFC-32 compositions, but increases at high HFC-32 compositions under the same condition.

Economic comparisons of HFC-32/HFO-1234yf mixtures to R-410A are shown in Figures 8 and 9 for heating and cooling modes, respectively. Positive values (no parentheses) indicate that the HFC-32/HFO-1234yf blend is economically favorable over R-410A. For heating mode at $T_{evap.}$ = −6.67 °C, the HFC-32/HFO-1234yf mixture becomes more economical than R-410A at w_{HFC-32} > 0.4 for capital cost and w_{HFC-32} > 0.5 for operating cost. Additional data at other evaporator temperatures are available in the Supporting Information (Figures S5 and S6).

https://doi.org/10.1021/acs.iecr.5c02778
Ind. Eng. Chem. Res. XXXX, XXX, XXX−XXX

For cooling mode at $T_{cond.}$ = 54.44 °C, the mixture is more favorable than R-410A at w_{HFC-32} > 0.4 (capital cost) and w_{HFC-32} > 0.6 (operating cost). The maximum economic benefit in both modes is observed at 100 wt % HFC-32. The Supporting Information includes additional results at $T_{cond.}$ = 32.22 and 43.33 °C (Figures S7 and S8).

A comparative summary of performance metrics including average C.O.P. values, operating and capital costs, and environmental performance is provided in Table 8. These results support the trends observed in Figures 8 and 9 that blends with higher HFC-32 composition, particularly R-454B and pure HFC-32, are higher efficiency, less expensive, and have reduced CO_2 emissions compared with R-410A and HFO-1234yf.

Table 8. Comparative Summary of Energy, Economic, and Environmental Performance Metrics for Refrigerant Candidates

refrigerant	average C.O.P. (cooling)	average C.O.P. (heating)	annual operating cost ($)	capital cost ($)	average TEWI (MT CO_2 per year)
R-410A	0.96	1.90	846	3500	178
HFC-32	1.12	2.04	709	2495	155
R-454B	1.04	1.97	792	2898	164
HFO-1234yf	0.85	1.83	928	4697	190

The capital cost was scaled using mass flow rate, but did not include differences in heat transfer coefficients as shown in Figures 10 and 11. Mixture compositions of HFC-32 and HFO-1234yf with higher heat transfer coefficients would reduce the estimated capital cost.

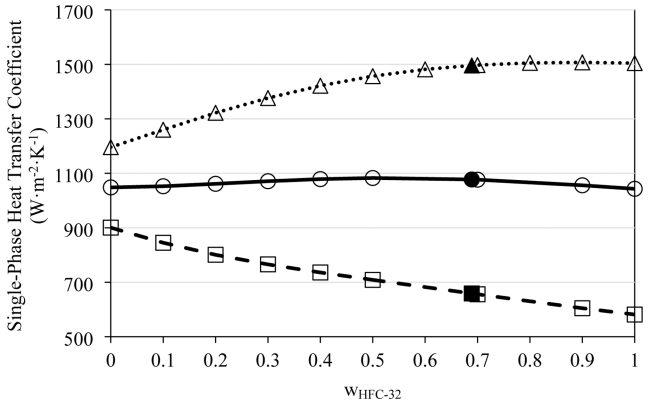

Figure 10. Single-phase heat transfer coefficients as a function of HFC-32 composition with h_{LS} (dotted line), h_{GS} (dashed line), and the arithmetic average of h_{LS} and h_{GS} (solid line) at evaporator temperature of $T_{evap.}$ = −1.11 °C. Solid symbols represent the composition for R-454B.

The cost analysis is based on a 10.5 kW residential-scale heat pump system. While relative trends should apply across differing capacities, savings will scale with both system size and regional electricity prices. In regions with higher electricity cost, operating cost reductions from high-COP blends become even more prominent. However, there are barriers to widespread adoption, as retrofitting existing systems utilizing R-410A may require hardware changes, and capital cost savings must be compared with retrofit for use of A2L refrigerants such as HFC-32 and mixtures of HFC-32 and HFO-1234yf.

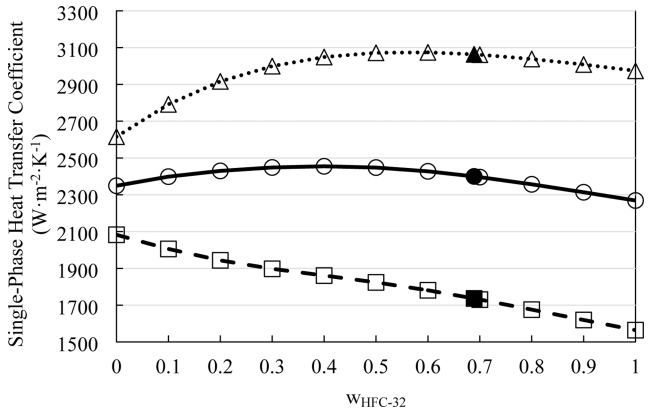

Figure 11. Single-phase heat transfer coefficients as a function of HFC-32 composition with h_{LS} (dotted line), h_{GS} (dashed line), and the arithmetic average of h_{LS} and h_{GS} (solid line) at condenser temperature of $T_{cond.}$ = 43.33 °C. Solid symbols represent the composition for R-454B.

Single-phase heat transfer coefficients for the liquid phase (h_{LS}) and vapor phase (h_{GS}) were calculated using the Dittus−Boelter correlation as shown in eqs 11 and 12[14]

$$h_{LS} = 0.034 \mathrm{Re}_{LS}^{0.8} \mathrm{Pr}_{L}^{0.4} \frac{\kappa_L}{D} \tag{11}$$

$$h_{GS} = 0.023 \mathrm{Re}_{GS}^{0.8} \mathrm{Pr}_{G}^{0.4} \frac{\kappa_G}{D} \tag{12}$$

where Re is the Reynolds number ($\mathrm{Re} = \frac{\rho v D}{\mu}$), Pr is the Prandl number ($\mathrm{Pr} = \frac{\mu C_p}{\kappa}$), and D is the tube diameter, assumed to be 0.01 m. Property values (thermal conductivity of the liquid κ_L, thermal conductivity of the gas κ_G, refrigerant density ρ,refrigerant velocity v, refrigerant viscosity μ) were obtained for vapor qualities of x = 0 and x = 1. Heat transfer coefficients at selected conditions are shown in Tables 9 and 10.

Table 9. Single-Phase Heat Transfer Coefficients for HFC-32/HFO-1234yf Mixtures at $T_{evap.}$ = −1.11 °C

mass fraction (w_{HFC-32})	h_{LS} at x = 0 (W·m^{-2}·K^{-1})	h_{GS} at x = 1 (W·m^{-2}·K^{-1})	average of h_{LS} and h_{GS} (W·m^{-2}·K^{-1})
0	1195.9	900.6	1048.3
0.689	1495.9	658.9	1077.4
1	1504.5	581.7	1043.1

Table 10. Single-Phase Heat Transfer Coefficients for HFC-32/HFO-1234yf Mixtures at $T_{cond.}$ = 43.33 °C

mass fraction (w_{HFC-32})	h_{LS} at x = 0 (W·m^{-2}·K^{-1})	h_{GS} at x = 1 (W·m^{-2}·K^{-1})	average of h_{LS} and h_{GS} (W·m^{-2}·K^{-1})
0	2615.9	2082.5	2349.2
0.689	3063.2	1736.4	2399.9
1	2973.9	1564.2	2269.0

The h_{LS} increases and h_{GS} decreases with increasing HFC-32 concentration during both condensation and evaporation as shown in Figures 10 and 11. The arithmetic average for h_{LS} and h_{GS} is also plotted to illustrate overall heat transfer performance. Overall, R-454B exhibits slightly higher heat transfer coefficients compared to pure HFC-32 at these operating conditions. Additional results at other temperatures can be found in the Supporting Information (see Figures S9−S12).

https://doi.org/10.1021/acs.iecr.5c02778
Ind. Eng. Chem. Res. XXXX, XXX, XXX−XXX

Environmental Impact. The annual CO_2 emissions for R-410A, HFC-32, and R-454B in a 10.5 kW (3 ton) heat pump system were calculated considering both direct emissions from refrigerant leakage and indirect emissions from energy consumption using the Total Equivalent Warming Impact (TEWI) approach.[15]

Direct CO_2 emissions were calculated based on the GWP of each refrigerant. For refrigerant mixtures, the GWP was calculated based on mass-weighted average of HFC-32 and HFO-1234yf, as shown in eq 13.

$$\mathrm{GWP}_{\mathrm{mixture}} = w_{\mathrm{HFC-32}} \times \mathrm{GWP}_{\mathrm{HFC-32}} + w_{\mathrm{HFO-1234yf}} \times \mathrm{GWP}_{\mathrm{HFO-1234yf}} \quad (13)$$

Depending on the choice of refrigerant and assumed leak volume (3 to 6 kg per year), direct CO_2 emissions ranged from 1.5 to 2025 kg (0.002 to 2 t, MT) for the lower-leak scenario and 3 to 4050 kg (0.003 to 4 t, MT) for the higher-leak scenario.

Indirect CO_2 emissions were calculated by estimating electricity use based on compressor power in each operating mode ($\mathrm{Po}_{\mathrm{mode}}$) and average run time of a unit. Daily energy usage was multiplied by seasonal operation time (~2160 h for cooling and heating modes), and converted to CO_2 emissions using an estimated average U.S. electricity emission factor (β) of 0.4 kg of CO_2 per kWh, as shown in eq 14.[16]

$$E_{\mathrm{mode,annual}} = \left(\frac{\mathrm{Po}_{\mathrm{mode}}}{60}\right) \times \frac{\mathrm{hours}}{\mathrm{day}} \times \frac{\mathrm{days}}{\mathrm{month}} \times \mathrm{months\ in\ mode} \quad (14)$$

The TEWI was evaluated on an annual basis as the sum of the direct emissions and indirect emissions, as shown in eq 15.

$$\mathrm{TEWI}_{\mathrm{annual}} = M_{\mathrm{leak}} \times \mathrm{GWP} + (E_{\mathrm{cool,annual}} + E_{\mathrm{heat,annual}}) \times \beta \quad (15)$$

The annual TEWI for HFC-32/HFO-1234yf compared to R-410A as a function of refrigerant leak rates is shown in Figure 12. At low HFC-32 compositions ($w_{\mathrm{HFC-32}}$ = 0.0 to 0.3), total CO_2 emissions exceed those of R-410A by up to 20 t per year, primarily due to higher direct emissions. For compositions above $w_{\mathrm{HFC-32}}$ = 0.3 to 0.5, TEWI becomes lower than R-410A, with reductions up to 28 t per year.

With approximately 375 million HVAC units in the U.S., switching to R-454B or HFC-32 could reduce CO_2 emissions by 7−10 billion metric tons annually.[17] Globally, there are an estimated 2 billion units, with potential emission reductions reaching 37−54 billion metric tons per year.[18]

These results highlight the significance of refrigerant choice to reduce environmental impacts based on both direct and indirect effects. In this study, indirect emissions account for ~98% of total CO_2 emissions; therefore, regulatory agencies should consider the energy efficiency for alternatives and not simply focus on the direct effect and GWP of a refrigerant. In systems without leaks, indirect effects account for 100% of the global warming effect, meaning that alternative refrigerants with lower energy efficiency could do more harm than good for the environment. This highlights the necessity of optimizing both energy efficiency and refrigerant GWP to reduce overall environmental impact.

Economic Impact. An economic analysis was conducted to compare the annual operating costs of R-410A and mixtures of HFC-32 and HFO-1234yf in HVAC systems. To determine the energy usage for different regions across the U.S., an average electricity prices of $0.10, $0.15, and $0.20 were used. The annual operating cost was calculated based on six months of cooling and six months of heating.

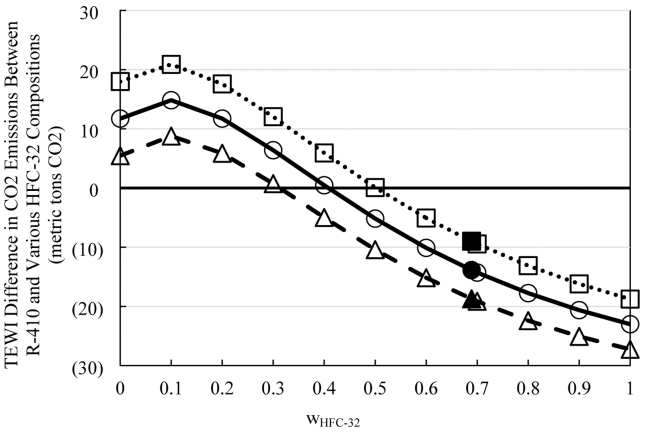

Figure 12. Comparison of the TEWI difference in annual CO_2 emissions (metric tons) between R-410A and mixtures of HFC-32 and HFO-1234yf as a function of refrigerant leak rate (triangles, no leakage; circles, 3 kg leak per year; and squares, 6 kg leak per year) for cooling ($T_{\mathrm{cond.}}$ = 43.33 °C and $T_{\mathrm{evap.}}$ = −1.11 C) and heating operating conditions ($T_{\mathrm{evap.}}$ = −6.67 °C and $T_{\mathrm{cond.}}$ = 43.33 °C). Solid symbols represent the R-454B composition. Positive values (no parentheses) and negative values (with parentheses).

To analyze savings, the total cost for each refrigerant mixture was compared to R-410A, by subtracting R-410A's cost from the alternative's total cost, as shown in Figure 13.

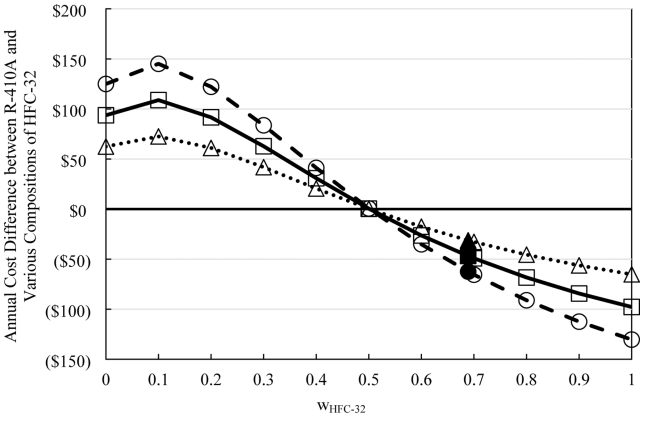

Figure 13. Difference in the annual costs of R-410A and HFC-32/HFO-1234yf at different prices for one kilowatt-hour: $0.10 (dotted line), $0.15 (solid line), $0.20 (dashed line). Solid symbols represent the R-454B composition. Positive values (no parentheses) and negative values (with parentheses).

For compositions of $w_{\mathrm{HFC-32}}$ = 0.1 to 0.3, annual costs exceed those of R-410A with a maximum cost difference of $70 to $145 occurring around $w_{\mathrm{HFC-32}}$ = 0.1. As the composition of HFC-32 increases, the cost difference decreases, indicating that the alternative refrigerant mixtures such as R-454B and HFC-32 will offer cost savings compared with R-410A. In fact, mixture compositions containing $w_{\mathrm{HFC-32}}$ = 0.5 to 1.0 offer cost savings relative to R-410A. The economic impact of refrigerant selection across the U.S. and globally could result in $54 to $290 billion in annual savings, respectively. Refrigerant choice

https://doi.org/10.1021/acs.iecr.5c02778
Ind. Eng. Chem. Res. XXXX, XXX, XXX−XXX

not only has an environmental impact, but also offers major economic benefits, particularly in regions with high electricity costs.

Safety is an important consideration in practical applications of HFC-32 and HFO-1234yf, which are both classified as mildly flammable (A2L) refrigerants under ASHRAE Standard 34. An increased HFC-32 in the refrigerant blend has been shown to increase burning velocity and flammability, although all mixtures are classified as A2L.[19] Flammability impacts refrigerant charge amount, system installation methods, and compliance with building codes. ASHRAE Standard 15 specifies leak prevention methods and ventilation requirements that must be followed. While these measures might slow adoption compared to nonflammable refrigerants, ongoing regulation and equipment designed specifically for A2L refrigerants are expected to address these challenges.

This study assumes evaporator and condenser temperatures applicable for air-conditioning and heat pump applications. Actual systems experience fluctuating ambient temperatures, loads, and seasonal changes that can impact energy efficiency and refrigerant performance. The use of average U.S. electricity prices provided a basis for comparison, but energy costs can vary by region and time of day, which could impact the cost-effectiveness of some refrigerants. Leakage rates were also generalized, although leakage rates can vary from system to system due to design and maintenance practices. Environmental regulations can also vary depending on the region. Both of these caveats can impact environmental analyses. Future work will include a life cycle analysis that will account for these scenarios.

CONCLUSION

Mixtures of HFC-32 and HFO-1234yf such as R-454B and pure HFC-32 show promise as alternatives to R-410A in heating and cooling applications. Thermodynamic and heat transfer modeling, combined with economic analysis, provide insight into how refrigerant mixtures with a higher HFC-32 composition increase C.O.P. and reduce capital and operating costs. Switching to R-454B and HFC-32 can reduce annual CO_2 emissions by 10−15%, and energy costs by 5−11% compared to R-410A, respectively. The global use of these refrigerants could prevent billions of metric tons of CO_2 emissions and result in significant economic savings. Subsequently, these results offer important information about refrigerant formulation and transition strategies, further emphasizing the necessity of high-efficiency, low-GWP refrigerant mixtures. Currently, there are two options available for replacing R-410A in air-conditioning and heat pump applications: R-454B and HFC-32. In addition, mixtures of HFC-32 and HFO-1234yf that contain 50 wt % or more HFC-32 can offer performance, environmental, and economic benefits compared with R-410A. Interestingly, while pure HFC-32 offers the best thermodynamic performance, heat transfer modeling indicates that R-454B offers advantages in condensation and evaporation compared with HFC-32. Future evaluations should combine both the thermodynamic and heat transfer effects to assess the overall performance, economic, and environmental impact advantages of HFC-32/HFO-1234yf mixtures compared with R-410A.

ASSOCIATED CONTENT

Supporting Information

The Supporting Information is available free of charge at https://pubs.acs.org/doi/10.1021/acs.iecr.5c02778.

Pressure-enthalpy diagrams, heat transfer data, cost comparisons, single-phase heat transfer coefficients, and operating conditions for HFC-32, HFO-1234yf, and their mixtures (PDF)

AUTHOR INFORMATION

Corresponding Author

Mark B. Shiflett − *Environmentally Applied Refrigerant Technology Hub (EARTH), U.S. National Science Foundation Engineering Research Center, University of Kansas, Lawrence, Kansas 66045, United States; Wonderful Institute for Sustainable Engineering, University of Kansas, Lawrence, Kansas 66045, United States; Department of Chemical and Petroleum Engineering, University of Kansas, Lawrence, Kansas 66045, United States;* orcid.org/0000-0002-8934-6192; Email: Mark.B.Shiflett@ku.edu

Authors

Clarice M. Sabolay − *Environmentally Applied Refrigerant Technology Hub (EARTH), U.S. National Science Foundation Engineering Research Center, University of Kansas, Lawrence, Kansas 66045, United States; Wonderful Institute for Sustainable Engineering, University of Kansas, Lawrence, Kansas 66045, United States; Department of Chemical and Petroleum Engineering, University of Kansas, Lawrence, Kansas 66045, United States;* orcid.org/0009-0008-5288-1205

Lokesh S. Valluru − *Environmentally Applied Refrigerant Technology Hub (EARTH), U.S. National Science Foundation Engineering Research Center, University of Kansas, Lawrence, Kansas 66045, United States; Wonderful Institute for Sustainable Engineering, University of Kansas, Lawrence, Kansas 66045, United States; Department of Chemical and Petroleum Engineering, University of Kansas, Lawrence, Kansas 66045, United States*

Complete contact information is available at: https://pubs.acs.org/10.1021/acs.iecr.5c02778

Notes

The authors declare no competing financial interest.

ACKNOWLEDGMENTS

This research is based upon work supported by the U.S. National Science Foundation under award number ERC-2330175 for the Engineering Research Center Environmentally Applied Refrigerant Technology Hub (EARTH).

NOMENCLATURE

Symbols

C.C.	capital cost ($)
C.O.P.	coefficient of performance
FRR	flow rate ratio
H	enthalpy ($kJ \cdot kg^{-1}$)
$\dot{m}$	mass flow rate ($kg \cdot min^{-1}$)
O.C.	operating cost ($\$ \cdot month^{-1}$)
MT	metric ton (1000 kg)
P	pressure (MPa)

https://doi.org/10.1021/acs.iecr.5c02778
Ind. Eng. Chem. Res. XXXX, XXX, XXX−XXX

Po	power ($kJ \cdot min^{-1}$)
$\dot{Q}$	heat transfer rate ($kJ \cdot min^{-1}$)
S	entropy ($kJ \cdot kg^{-1} \cdot K^{-1}$)
T	Temperature (°C or K)
w_{HFC-32}	mass fraction of HFC-32
Re	reynolds number
Pr	prandtl number
D	diameter (m)

Greek Letters

κ	thermal conductivity ($W \cdot m^{-1} \cdot K^{-1}$)
μ	dynamic viscosity (Pa·s)
υ	velocity ($m \cdot s^{-1}$)
ρ	density ($kg \cdot m^{-3}$)

Subscripts and Superscripts

cond	condenser
evap	evaporator
LS	liquid phase
GS	gas phase
mix	mixture
sat	saturated state
SC	subcooled
SH	superheated

Abbreviations

AIM Act	American Innovation and Manufacturing Act
GWP	global warming potential
HC	hydrocarbon
HCFC	hydrochlorofluorocarbon
HFC	hydrofluorocarbon
HFO	hydrofluoroolefin
HVAC	heating, ventilation, and air conditioning,
MC	manufacturer's cost
NIST	National Institute of Standards and Technology
ODP	ozone depletion potential
REFPROP	reference fluid thermodynamic and transport properties database
TEWI	total equivalent warming impact
VC	vapor-compression

REFERENCES

(1) Domanski, P. A.; Brignoli, R.; Brown, J. S.; Kazakov, A. F.; McLinden, M. O. Low-GWP Refrigerants for Medium and High-Pressure Applications. *Int. J. Refrig.* **2017**, *84*, 198−209.

(2) Alsouda, F.; Bennett, N. S.; Saha, S. C.; Salehi, F.; Islam, M. S. Vapor Compression Cycle: A State-of-the-Art Review on Cycle Improvements, Water and Other Natural Refrigerants. *Clean Technol.* **2023**, *5*, 584−608.

(3) Powell, R. L. CFC Phase-Out: Have We Met the Challenge? *J. Fluorine Chem.* **2002**, *114* (2), 237−250.

(4) Arishi, A. M.; Espinoza Mejia, J. E.; Shiflett, M. B. Separation of Azeotropic Refrigerant Mixtures: R-450A, R-456A, R-515B, and R-516A Using Phosphonium- and Imidazolium-Based Ionic Liquids. *Ind. Eng. Chem. Res.* **2024**, *63*, 6754−6765.

(5) United Nations Environment Programme. *2018 Report of the Refrigeration, Air Conditioning, and Heat Pumps Technical Options Committee*; UNEP: Nairobi, 2018. https://ozone.unep.org/sites/default/files/2019-04/RTOC-assessment-report-2018_0.pdf.

(6) Nair, V. HFO Refrigerants: A Review of Present Status and Future Prospects. *Int. J. Refrig.* **2021**, *122*, 156−170.

(7) Kadhim, S. A.; Al-Ghezi, M. K. S.; Ashour, A. M. Theoretical Analysis of Energy, Exergy, and Environmental-Related Aspects of Hydrofluoroolefin Refrigerants as Drop-In Alternatives for R134a in a Household Refrigerator. *J. Therm. Sci. Eng. Appl.* **2025**, *17*, 021003.

(8) Abedsoltan, H.; Shiflett, M. B. Transitioning to a Lower Global Warming Refrigerant, A Performance Study of R-513A and HFC-134a in Commercial Chillers. *Ind. Eng. Chem. Res.* **2024**, *63* (49), 21603−21612.

(9) Kadhim, S. A. Thermodynamic and Environmental Analysis of Hydrocarbon Refrigerants as Alternatives to R-134a in Domestic Refrigeration. *Int. J. Thermodyn.* **2024**, *27* (2), 10−18.

(10) Ashour, A. M.; Kadhim, S. A.; Jaffar, H. M.; Ibrahim, O. A. A.-M.; Mota-Babiloni, A.; Bouabidi, A. Experimental Investigation of the Performance of Vapor Compression Cycle in a Water Cooler System with Low-GWP Alternative Refrigerants. *Therm. Sci. Eng. Prog.* **2025**, *62*, 103611.

(11) Zaki, O. M.; Abdelaziz, O. Critical Assessment of R-410A Alternatives for Mini-Split Air Conditioners in the Egyptian Market. *Energy Built Environ.* **2024**, *5* (3), 426−445.

(12) Selbaş, R.; Kızılkan, Ö.; Şencan, A. Thermoeconomic Optimization of Subcooled and Superheated Vapor Compression Refrigeration Cycle. *Energy* **2006**, *31* (12), 2108−2128.

(13) Lemmon, E. W.; Bell, I. H.; Huber, M. L.; McLinden, M. O. *NIST Standard Reference Database 23: Reference Fluid Thermodynamic and Transport Properties—REFPROP, Version 10.0*; National Institute of Standards and Technology, Standard Reference Data Program: Gaithersburg, MD, 2018.

(14) Shah, M. M.; Thome, J. R. A General Correlation for Heat Transfer during Film Condensation in Mini-Channels and Micro-channels. *Int. J. Heat Mass Transfer* **1979**, *22* (4), 547−556.

(15) IPCC; UNEP. *IPCC/TEAP Special Report on Safeguarding the Ozone Layer and the Global Climate System: Issues Related to Hydrofluorocarbons and Perfluorocarbons, Summary for Policymakers and Technical Summary*, 2005.

(16) U.S. Energy Information Administration (EIA). Frequently Asked Questions (FAQs). https://www.eia.gov/tools/faqs/faq.php?id=74&t=11 (accessed 2025−05−02).

(17) International Energy Agency. *Future of Cooling: Opportunities for Energy-Efficient Air Conditioning*; International Energy Agency: Paris, 2018. https://iea.blob.core.windows.net/assets/0bb45525-277f-4c9c-8d0c-9c0cb5e7d525/The_Future_of_Cooling.pdf (accessed 2025−05−02).

(18) International Energy Agency. *Space Cooling*; https://www.iea.org/energy-system/buildings/space-cooling (accessed 2025−05−02).

(19) Sadaghiani, M. S.; Arami-Niya, A.; Zhang, D.; Tsuji, T.; Tanaka, Y.; Seiki, Y.; May, E. F. Minimum Ignition Energies and Laminar Burning Velocities of Ammonia, HFO-1234yf, HFC-32 and Their Mixtures with Carbon Dioxide, HFC-125 and HFC-134a. *J. Hazard. Mater.* **2021**, *407*, 124781.

https://doi.org/10.1021/acs.iecr.5c02778
Ind. Eng. Chem. Res. XXXX, XXX, XXX−XXX